
This is an electronic reprint of the original article.
This reprint may differ from the original in pagination and typographic detail.

Hassanzada, Q.; Sarsari, I. Abdolhosseini; Hashemi, A.; Ghojavand, A.; Gali, A.; Abdi, M.
Theoretical study of quantum emitters in two-dimensional silicon carbide monolayers

Published in:
Physical Review B

DOI:
[10.1103/PhysRevB.102.134103](https://doi.org/10.1103/PhysRevB.102.134103)


Published: 07/10/2020

Document Version
Publisher's PDF, also known as Version of record

Please cite the original version:

Hassanzada, Q., Sarsari, I. A., Hashemi, A., Ghojavand, A., Gali, A., & Abdi, M. (2020). Theoretical study of quantum emitters in two-dimensional silicon carbide monolayers. *Physical Review B*, 102(13), 1-8. Article 134103. <https://doi.org/10.1103/PhysRevB.102.134103>

Theoretical study of quantum emitters in two-dimensional silicon carbide monolayers

Q. Hassanzada,¹ I. Abdolhosseini Sarsari ,¹ A. Hashemi,² A. Ghojavand,¹ A. Gali,³ and M. Abdi¹

¹*Department of Physics, Isfahan University of Technology, Isfahan 84156-83111, Iran*

²*Department of Applied Physics, Aalto University, FI-00076 Aalto, Finland*

³*Department of Atomic Physics, Budapest University of Technology and Economics, Budafoki út 8, 1111 Budapest, Hungary*



(Received 18 February 2020; revised 5 July 2020; accepted 21 September 2020; published 7 October 2020)

The electronic and optical features of some potential single-photon sources in two-dimensional silicon carbide monolayers is studied via *ab initio* calculations and group theory analyses. A few point defects in three charge states (negative, positive, and neutral) are considered. By applying performance criteria, Stone-Wales defects without and with combination of antisite defects are studied in detail. The formation energy calculations reveal that neutral and positive charge states of these defects are stable. We compute the zero-phonon-line energy, the Huang-Rhys (HR) factor, and the photoluminescence spectrum for the available transitions in different charge states. The calculated HR values and the related Debye-Waller factors guarantee that the Stone-Wales defects have a high potential of performing as a promising single-photon emitter.

DOI: [10.1103/PhysRevB.102.134103](https://doi.org/10.1103/PhysRevB.102.134103)

I. INTRODUCTION

Two-dimensional (2D) materials have recently received much attraction in the scientific communities because of their unique properties and extensive applications. A prominent aspect of 2D materials is their applications in quantum technologies where single photons are essential. Observation and investigation of single photons in 2D materials such as *h*-BN, transition metal dichalcogenides, WO₃, and GaSe [1–7], has raised a great interest toward this class of materials in the field of single-photon emitters (SPEs). SPEs in 2D materials are applicable in many quantum technologies ranging from quantum nanophotonics to quantum sensing and quantum information processing [8]. In such materials, the 2D nature of the host considerably improves the photon-extraction efficiency, provides more control over the defect implantation techniques, eases coupling to the waveguides, and provides compatibility with other 2D materials [9]. These advantages have inspired researchers to search and find 2D materials in which all the desired properties of an efficient single-photon source are met. Over the past few years, group IV semiconductors have shown significant potential to host SPEs, in such a way that most ideal single-photon sources were investigated just in diamond and silicon carbide (SiC) [10,11]. Among these traditional three-dimensional (3D) bulk materials, SiC not only emits room temperature single photons but also provides the brightest nonclassical light ever [12,13]. The advantages of 3D SiC in hosting SPEs makes one consider the investigation of the local point defects in its 2D form as potential color centers.

Even though the fabrication of 2D-SiC is still challenging [14–18], the recent observation of SiC nanograin assembly in graphene oxide pores [18] and investigation of quasi-two-dimensional SiC [17] affirm that the fabrication of two-dimensional SiC is about to emerge. Besides, theoretical calculations reveal that many possible 2D structures of SiC

are probable in which Si_{0.5}C_{0.5} structure is the most stable one [19]. Despite the preference of *sp*³ hybridization of the Si atoms, the Si_{0.5}C_{0.5} structure, which here on we call 2D-SiC, is predicted to be flat with *sp*² hybrid bonds. The band gap of this structure is larger than 3 eV making it an appropriate host for color centers. Considering the high potential of bulk SiC in producing color centers, the predicted wide band gap of 2D-SiC and the superiority of 2D materials in some applications, defects in two-dimensional SiC are expected to be capable of emitting ideal single photons.

In this work we present a study on electronic and optical properties of some favorable defects in 2D-SiC utilizing first-principles calculations assisted by group theoretical analysis to explore SPEs. The study includes vacancy, antisite, substitutional, and Stone-Wales (SW) defects. To investigate potential quantum emission defects, we first calculate zero-phonon-line (ZPL) energy for all possible transitions. Afterwards, we evaluate the Huang-Rhys (HR) factor and the related photoluminescence (PL) spectrum for the most likely cases. Our first-principles study reveals that the family of SW defects—SW (a simple 90° rotation of a silicon-carbon pair), SW-Si_C (a silicon-carbon pair rotation with silicon instead of carbon), and SW-C_{Si} (a silicon-carbon pair rotation with carbon instead of silicon)—have a high potential for emitting high-quality single photons. The results of this work serve in speeding up the understanding and identification of color centers in hexagonal structure of SiC, once realized experimentally. Our analyses and computations directly apply to the freestanding monolayers. Nonetheless, the results are applicable to the case where the layer is positioned on a proper substrate with slight modifications in their properties.

This paper is divided into five sections. The first section gives a brief overview of single-photon emitting in SiC systems. Section II discusses the first-principles and group theoretical methods for finding the most promising

single-photon emitters in the two-dimensional silicon carbide. Section III, the results and discussions, examines zero-phonon-line energy, Huang-Rhys factor, and the photoluminescence spectrum for the selected defects in 2D-SiC. Our conclusions and outlook are drawn in the final section.

II. METHOD

To analyze point defects embedded in 2D-SiC, density functional theory (DFT) is used as implemented in the VASP code [20]. The electronic structure is calculated using the generalized gradient approximation by Perdew, Burke, and Ernzerhof (PBE) [21]. Since isolated defects embedded in a wide band gap material cause isolated states inside the band gap, the initial step is to calculate the band gap correctly. Due to the well-known failure of DFT in the calculation of the band gap, the hybrid exchange functional of Heyd, Scuseria, and Ernzerhof (HSE06) is applied to overcome this problem [22,23].

The motivation behind HSE06 hybrid functionals is the observation that Hartree-Fock overestimates band gaps and semilocal density functionals underestimate them. Therefore by mixing the two methods with appropriate weights, one gets intermediate reliable results. The HSE06 hybrid functional calculates the band gap and the charge transition levels of group-IV semiconductors within 0.1 eV accuracy [24].

The excited-state calculations are carried out using the constrained-occupation DFT (CDFT) approach which gives reliable results for the ZPL energy when compared to experimental data [25]. In the CDFT method, the constraint is done by adding a Lagrange multiplier term to the traditional DFT energy functional. This constraint enforces the desired charge or spin states for the specified regions of atoms [26]. Implementing this method in different simulation packages such as VASP, Quantum Espresso, and GPAW. It is widely used in the study of single-photon emitters as a standard excitation method. The validity of this method has been verified by calculation of the optical properties of group-IV vacancy color centers in diamond [25]. In using the CDFT, one electron from an occupied and localized state is promoted to a higher unoccupied and localized state inside the band gap, and it is held in the excited state while the atomic positions are relaxed. The total energy difference between the optimized ground state and the mentioned excited state then gives the approximate value of the ZPL energy. It is worth mentioning that, in the calculation of ZPL energy of defects in semiconductors, one has to use a large enough supercell to avoid self-interaction of defects.

Because of the limited computational resources at hand, a supercell of 72 atoms (6×6) is chosen to conduct preliminary research on the electronic structure of different defects. When a few candidates are handpicked, the supercell size is magnified to 128 atoms (8×8) to study the convergence of the calculations. For 6×6 supercell a vacuum of 12 Å and for 8×8 supercell a vacuum of 24 Å are considered to separate the periodic images. Note that this indeed implies a freestanding structure of 2D-SiC. Nonetheless, the results remain applicable with slight modifications in the electronic and magnetic properties of the point defects for the case of 2D-SiC on a proper substrate, where the layer weakly bonds

to the substrate surface. A single k point (Γ point) is applied to sample the Brillouin zone. While a single k point might not be numerically convergent for a supercell of 72 atoms, the obtained results serve as a guidance to pick up the most likely candidates for further investigations. An energy cutoff of 450 eV is utilized for the plane-wave basis set within the projector augmented-wave method (PAW) [27,28]. The ground state electronic structure is obtained by performing geometry relaxation in which internal positions of atoms are relaxed until forces on them are smaller than 0.02 eV/Å. Within the CDFT method, the ions are relaxed to reach the global minimum of adiabatic potential energy surface in the excited state.

The PL spectrum is calculated within the HR theory which was proposed by Huang and Rhys in 1950 [29]. One important quantity in HR theory is the partial Huang-Rhys factor. This factor helps us in assessing a point defect as a good single-photon emitter. The factor is given by

$$S_k = \frac{\omega_k q_k^2}{2\hbar}, \quad (1)$$

where ω_k is frequency of the k th phonon mode, \hbar is the reduced Planck constant, and q_k is defined as

$$q_k = \sum_{\alpha,i} m_\alpha^{1/2} (R_{\alpha,i}^{(e)} - R_{\alpha,i}^{(g)}) \Delta r_{k,\alpha,i}, \quad (2)$$

where m_α is the mass of atom α , $R_{\alpha,i}^{(e)}$ and $R_{\alpha,i}^{(g)}$ are equilibrium atomic coordinate of atom α along the direction i in the excited state and the ground state, and $\Delta r_{k,\alpha,i}$ is the normalized displacement vector of atom α along the direction i in phonon mode k . Sum of the partial HR factor over all phonon modes k gives the total HR factor. This quantity determines coupling between electronic and vibrational states and characterizes the phonon side band. The PL intensity is defined as

$$L(\hbar\omega) = C\omega^3 A(\hbar\omega), \quad (3)$$

where C is the normalization constant and $A(\hbar\omega)$ is the optical spectral function given by

$$A(\hbar\omega) = \frac{1}{2\pi} \int_{-\infty}^{\infty} G(t) e^{i\omega t - \gamma|t|} dt. \quad (4)$$

Here γ is linewidth of the ZPL, $G(t)$ is the generating function and is defined as

$$G(t) = e^{S(t) - S_{\text{tot}}}, \quad (5)$$

where $S(t)$ is the Fourier transform of the partial HR factor, defined as

$$S(\hbar\omega) = \sum_k S_k \delta(\hbar\omega - \hbar\omega_k), \quad (6)$$

and S_{tot} is the total HR factor. The Debye-Waller (DW) factor describes the ratio of the emission of coherent photons vs total number of emitted photons including the phonon assisted ones which compromise the coherence. This factor is related to the HR factor and determines the weight of the ZPL.

Here the PL spectrum and the HR factor are calculated based on Refs. [30,31]. Since the PBE functional provides the PL spectrum in good agreement with the HSE06 hybrid functional, by applying this functional the geometry is relaxed

until all forces are smaller than 10^{-3} eV/Å, then density functional perturbation theory (DFPT) within the VASP code is used to obtain the phonon eigenfrequencies and eigenvectors. Calculation of the HR factor is very expensive due to its requirement to the full phonon spectrum. Therefore its calculations is not computationally affordable for all of the surveyed defects. For this reason, we single out a few most promising color center candidates in our search among the point defects by using their ΔQ parameter as a filtering parameter. The calculation of ΔQ is not computationally expensive, nonetheless, its behavior is proportional to that of the HR factor. In fact, ΔQ specifies the atomic structure change during the excitation. To calculate it, we apply one-dimensional configuration coordinate formulation which is represented by

$$\Delta Q^2 = \sum_{\alpha,i} m_{\alpha} \Delta R_{\alpha,i}^2, \quad (7)$$

where $\Delta R_{\alpha,i}$ is $R_{\alpha,i}^{(e)} - R_{\alpha,i}^{(g)}$. As mentioned above, the high (low) values of ΔQ correspond to high (low) values of the HR factor. The stability of charged defects is determined by evaluating the formation energy as a function of the Fermi level as [32]

$$E_q^F(\epsilon_f) = E_{\text{SiC},q}^{\text{tot}} - E_{\text{SiC},p} + q[\epsilon_{\text{vbm}}^{\text{pri}} + \epsilon_F - \Delta V_{0/p}] - n_x \mu_x + E_q^{\text{corr}}. \quad (8)$$

In the above equation, E_q^{tot} is the total energy of the 2D-SiC supercell containing the charged defects, $E_{\text{SiC},p}$ and $\epsilon_{\text{vbm}}^{\text{pri}}$ are the total energy of a pristine 2D-SiC and pristine valence band maximum, μ_x is the chemical potential of atoms and n_x determines the number of atom of type x added (positive) or removed (negative) from the pristine supercell, and E_q^{corr} is the finite-size electrostatic correction.

$\Delta V_{0/p}$ is an aligning term which aligns the electrostatic potentials of pristine and defective supercells. We apply the correction term based on the FNV scheme [33], which is implemented in the CoFFEE code [34]. In this method E_q^{corr} is given by

$$E_q^{\text{corr}} = E_q^{\text{lat}} - q \Delta V_{q-0/m}, \quad (9)$$

where $E_q^{\text{lat}} = E_q^{\text{iso}} - E_q^{\text{per}}$ is the long range interaction energy which is obtained from solving the Poisson equation using a model charge distribution and a model dielectric profile. The dependence of E_q^{corr} on the model charge distribution is eliminated through $\Delta V_{q-0/m}$ which aligns the DFT difference potential to the model potential:

$$\Delta V_{q-0/m} = (V_q^{\text{DFT}} - V_0^{\text{DFT}})|_{\text{far}} - V_q^{\text{per},m}|_{\text{far}}. \quad (10)$$

The term ϵ_F in Eq. (8) determines the electrons added (for $q < 0$) or removed (for $q > 0$) from the defective supercell. Fermi level (ϵ_F) or chemical potential is considered as the energy of reservoir for electron exchange and is referenced to the valence-band maximum (VBM). The formation energies plotted in Fig 3 demonstrate the range of Fermi level in which a given charge state is stable (for every value of ϵ_F the charge state with the lowest formation energy is stable). The crossing points of these lines represent charge transition levels. For the growth condition, it is assumed that in the Si-rich condition,

TABLE I. The calculated ZPL energy and ΔQ value for defects possible transitions using a HSE06 hybrid functional in a 6×6 supercell. The superscripts “up” and “down” refer to spin up and spin down channels.

Defect	$E_{\text{ZPL}}^{\text{up}}$ (eV)	$E_{\text{ZPL}}^{\text{down}}$ (eV)	ΔQ (Å amu ^{1/2})
V_C^+	2.59	—	2.41
V_C^-	—	0.59	1.23
$V_{\text{Si}}-V_C$	0.917	—	1.25
	1.76	—	2.16
$V_{\text{Si}}-V_C^+$	1.02	—	1.56
	2.21	—	1.20
$V_{\text{Si}}-V_C^-$	—	1.51	1.08
V_C-C_{Si}	1.48	—	0.83
	1.05	—	0.85
$V_C-C_{\text{Si}}^+$	0.86	—	1.25
	1.69	—	0.88
	2.32	—	0.93
$V_C-C_{\text{Si}}^-$	—	2.18	0.63
	—	0.41	0.87
V_{Si}	—	1.99	1.03
	—	1.05	0.94
V_{Si}^+	—	0.88	0.58
	—	1.90	1.05
	—	1.97	1.11
V_{Si}^-	—	2.03	1.42
SW	1.47	—	0.46
SW^+	1.63	—	0.49
SW^-	—	1.60	0.53
$SW-Si_C$	1.54	—	0.39
$SW-Si_C^+$	1.77	—	0.40
	2.64	—	0.46
$SW-Si_C^-$	—	3.35	0.35
	—	3.29	0.22
	—	1.50	0.42
$SW-C_{\text{Si}}$	1.65	—	0.53
	1.32	—	2.32
	2.28	—	0.63
$SW-C_{\text{Si}}^+$	1.73	—	0.57
	1.33	—	2.51
	2.51	—	0.81
$SW-C_{\text{Si}}^-$	—	1.67	0.48

2D-SiC is in equilibrium with bulk Si, whereas in the C-rich condition it is in equilibrium with graphite.

In order to assist the DFT calculations, we invoke group theory analysis for further understanding of the electronic and spin properties of the studied point defects. As it will become clear shortly, the focus of our study is put on the Stone-Wales defect varieties. The molecular symmetry of these defects is relatively low as they assume either a C_{2v} - or C_s -point group symmetry. The molecular orbitals (MOs), which are a linear combination of the atomic orbitals, are formed by adapting the symmetry of the molecules. These MOs provide a basis that diagonalizes the configuration Hamiltonian. Each orbital has the symmetry of one irreducible representation (irr) of the point group. By investigating the character tables and comparing the MOs provided by the *ab initio* calculations, one identifies their irreducible representation. The multielectron states are then obtained by first determining the orbital

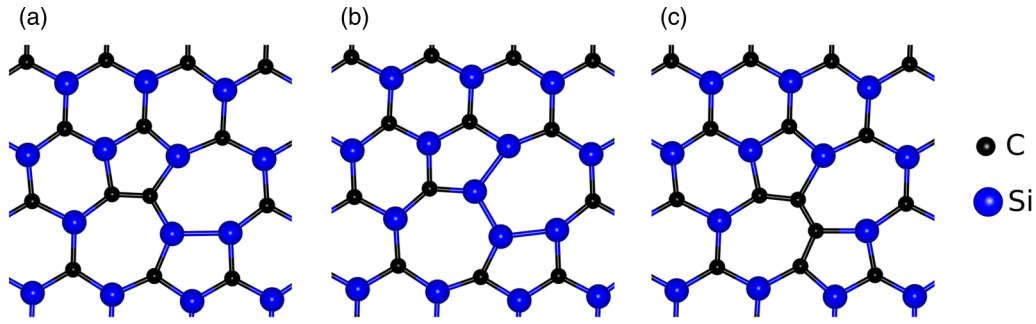


FIG. 1. Atomic structure of (a) SW, (b) SW-SiC, and (c) SW-CSi defects. Silicon and carbon atoms are illustrated by blue and black colors, respectively

occupations, and then the spin state of the collective electrons, and finally the tensor product of the spatial wave function with the spin part. Here the neutral charge defects can only assume singlet spinor in their ground state and both singlet and triplet states in the electronic excited state. All other combinations are rejected by Pauli's exclusion principle. Meanwhile, the positively charged defects are only spin doublet.

The group theory allows us to predict potentially nonzero matrix elements of the Hamiltonians that are perturbatively included in the analysis. The spin-orbit interaction is one of the crucial interactions that yet remains a perturbation in the system as SiC is composed of relatively light atom species. The interaction induces nonradiative transitions between the multielectron states. Another critical effect which lies at the heart of our analysis is the electric dipole interaction that determines dark and bright states. Those states that their dipole moment can couple to the ground state via the external electric field, provided by electromagnetic radiation, determine the selection rules [35,36]. In this part of study, the value of matrix elements $\langle \psi | O | \phi \rangle$ is vanishing if their total irreducible symmetry is not that of totally symmetric irreducible representation, here A_1 and A' for the C_{2v} and C_s , respectively. In the mathematical expression $\Gamma(\psi) \otimes \Gamma(O) \otimes \Gamma(\phi) \not\supset \Gamma_1$, where $\Gamma(X)$ is the irreducible representation of the object X and Γ_1 is the totally symmetric irr. The selection rules are obtained by studying the electric dipole interaction $H_{dp} = -\mathbf{d} \cdot \mathbf{E}$, where $\mathbf{d} = -e(x, y, z)$ is the dipole moment of the electronic state and \mathbf{E} is the electric field vector. \mathbf{d} transforms like a polar vector, and its components have a different irr as listed in the character tables. The polarization of radiative transitions is thus predicted by inspecting those components with nonvanishing matrix elements.

III. RESULTS AND DISCUSSIONS

In our DFT calculation we find that 2D-SiC remains in a plane which agrees with previous works [18,19]. The Si-C bond distance is calculated to be 1.78 Å with PBE functional and 1.77 Å with HSE06 hybrid functional. We evaluate a large band gap of 3.58 eV for 2D-SiC with HSE06 hybrid functional which is larger than any main polytypes of SiC. We survey various defects which are probable in 2D-SiC. These defects include Si/C vacancy, vacancy-antisite, divacancy, Si/C substitutional, and Stone-Wales defects (SW, SW-SiC, SW-CSi). Stone-Wales defects involve an in-plane 90° rotation of a bond in sp^2 -bonded materials. They already have been

investigated in graphene and silicene [14,16–18]. Due to this fact, their formation in 2D-SiC is expected. We study the defects electronic structure in a 6×6 supercell, inspecting their properties as a color center candidate. By looking for the electronic levels inside the band gap and the possible transitions between these levels for every defect, we find that both of SiC (silicon instead of carbon) and CSi (carbon instead of silicon) defects are inappropriate as they do not introduce any states within the band gap. On the other hand, the possible transitions of the neutral V_C defect exhibit small values of ZPL energy, putting them in the infrared region. We, therefore, exclude these defects from our further analysis. For all surveyed defects, we calculate the possible excited states within the CDFT approach. The results are summarized in Table I. We employ the ΔQ parameter to handpick the defects so that those defects with ΔQ parameters smaller than $0.6 \text{ Å amu}^{1/2}$ are considered for the detailed study. One clearly notices that Stone-Wales defects SW, SW-SiC, SW-CSi, and V_{Si}^+ satisfy this criterion. Even though it suggests that they could have the potential to emit single photons, further study is needed to confirm this speculation. Our focus is set on optical photon emitters. Thus, due to the small value of the ZPL energy for V_{Si}^+ defect, our investigation becomes restricted to the Stone-Wales defects. The atomic structure of these defects and the electronic structure of the few lowest states are shown in Figs. 1 and 2, respectively. We investigate the relative stability of these defects by computing the formation energy in neutral, negative, and positive charge states in a 8×8 supercell.

We consider SW-SiC defect as an example, and we show how we calculate the formation energy of this defect. According to Eq. (8), we first need to obtain the total energy of a supercell containing the charged SW-SiC defect ($E_{SiC,q}^{\text{tot}}$) and a pristine supercell of the same size ($E_{SiC,p}$). $\Delta V_{0/p}$, E_q^{corr} are calculated using CoFFEE code. $\epsilon_{vbm}^{\text{pri}}$ is evaluated from $\epsilon_{vbm}^{\text{pri}} = E_{\text{tot}}^{\text{pri}}(n) - E_{\text{tot}}^{\text{pri}}(n-1)$, where $E_{\text{tot}}^{\text{pri}}(n)$, $E_{\text{tot}}^{\text{pri}}(n-1)$ terms are the total energy of a pristine supercell in neutral and positive charge state, respectively. Since in this defect one silicon atom is added, and one carbon atom is removed, we have $\sum_x n_x \mu_x = \mu_{Si} - \mu_C$, where μ_{Si} is the chemical potential of silicon and μ_C is the chemical potential of carbon. The values of the chemical potentials depend on the growth conditions, so we calculate silicon and carbon chemical potentials in Si-rich and C-rich conditions. Because in Si-rich condition the system is in equilibrium with bulk silicon, the silicon chemical potential is obtained from bulk silicon (total energy

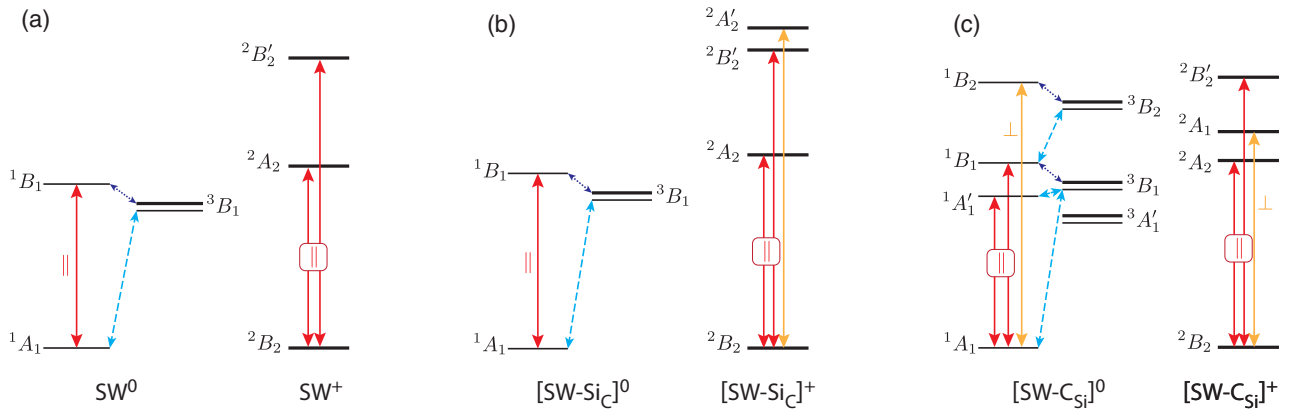


FIG. 2. The electronic structure (to the scale) of the three SW defects thoroughly studied in this work in the neutral and positive charge states. The solid arrows indicate allowed dipole transitions. The transitions with in-plane polarization are expected to give brighter emissions (red) while the transitions induced by the out-of-plane dipole moments are presented in orange (weaker excitation). Dashed and dotted blue arrows show the nonradiative transitions that can be induced by spin interactions.

per atom). Then the carbon chemical potential can be obtained from $\mu_{\text{SiC}} = \mu_{\text{Si}} + \mu_{\text{C}}$ where μ_{SiC} is the total energy of SiC primitive cell. In C-rich condition, the carbon chemical potential is derived from graphite (total energy per atom), and for the silicon chemical potential we use the equilibrium condition as explained. The results for HSE06 hybrid functional are presented in Fig. 3. The obtained formation energy shows that the negative charge state is not stable for any of the Stone-Wales defects as the (0/−) charge transition levels for SW, SW-SiC, and SW-CSi defects are at EV + 4.00, EV + 4.30, and EV + 4.19 eV, respectively, where EV is the valence band maximum. Unlike the negative charge states, the neutral charge states are stable as the (+/0) charge transition levels are at EV + 0.43, EV + 0.59, and EV + 0.23 eV, respectively. We also consider the positive charge state of these defects stable because their highest occupied molecular

orbital (HOMO) lies between the (+/0) charge transition level and the valence band maximum within the band gap.

One expects when the heat of formation of SiC-2D lattice is negative, the formation energy of SW-SiC (SW-CSi) defect in Si-rich (C-rich) condition to be lower in energy than in the C-rich (Si-rich) condition. But the trends obtained in Fig. 3 are opposite, and it is because the heat of formation of 2D-SiC is positive (0.56 eV) and this material is only a metastable form of silicon carbide. The heat of formation is obtained from $\Delta H_f = \mu_{\text{SiC}}^{2\text{D}} - (\mu_{\text{Si}}^{\text{bulk}} + \mu_{\text{C}}^{\text{graphite}})$ where $\mu_{\text{SiC}}^{2\text{D}}$ is the total energy of 2D-SiC primitive cell, $\mu_{\text{Si}}^{\text{bulk}}$ is the total energy per atom of bulk silicon, and $\mu_{\text{C}}^{\text{graphite}}$ is the total energy per atom of graphite [37]. Another point is that SW-CSi defect could be about 2 eV lower in formation energy than the SW-SiC defect in stoichiometric conditions, simply because the C atom likes the sp^2 configuration much more than the Si atom does. Thus, changing the C/Si ratio (Si-rich vs C-rich condition) does not alter this order but only closes the energy spacing.

Before going through the detailed *ab initio* calculation on these defects, we provide a group of theoretical calculations with an emphasize on the electronic structure and the possible transitions, both radiative and nonradiative. The substitutional SW defects have a C_{2v} symmetry and irr of their orbitals are as assigned in Fig. 4. The neutral charge defects have a fully occupied singlet orbital in their ground state. Thus, we expect a spin-singlet state for these cases. In the excited states, however, both singlet and triplet spin states are allowed that divides the radiative transition channels into triplet and singlet as the dipole transitions are spin state preserving in the zeroth order of spin-orbit Slater states. This allows us to construct the electronic structure of the few lowest states and determine the polarization of the radiative transitions according to the matrix element symmetries (see Fig. 2 for the structure as well as the transitions). The positively charged defects provide only one electron in the band gap, which implies the one have to expect spin-doublet states. We find that the order of orbitals is slightly shuffled by subtraction of one electron from the defect. The electronic structure, thus, behaves differently. Our analysis on the spin-orbit interaction suggests that nonradiative transition through the shelving states is also possible. The

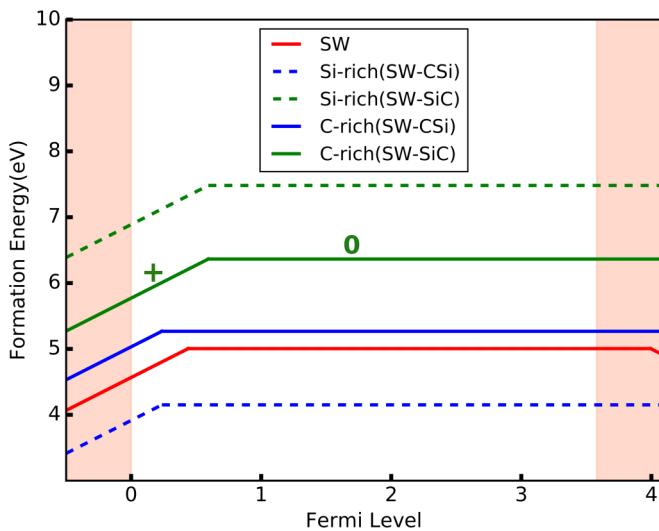


FIG. 3. Formation energy as a function of the Fermi level for SW (red lines), SW-SiC (green lines), and SW-CSi (blue lines) defects in C-rich (solid lines) and Si-rich (dashed lines) growth conditions. Both growth conditions for SW defect are the same.

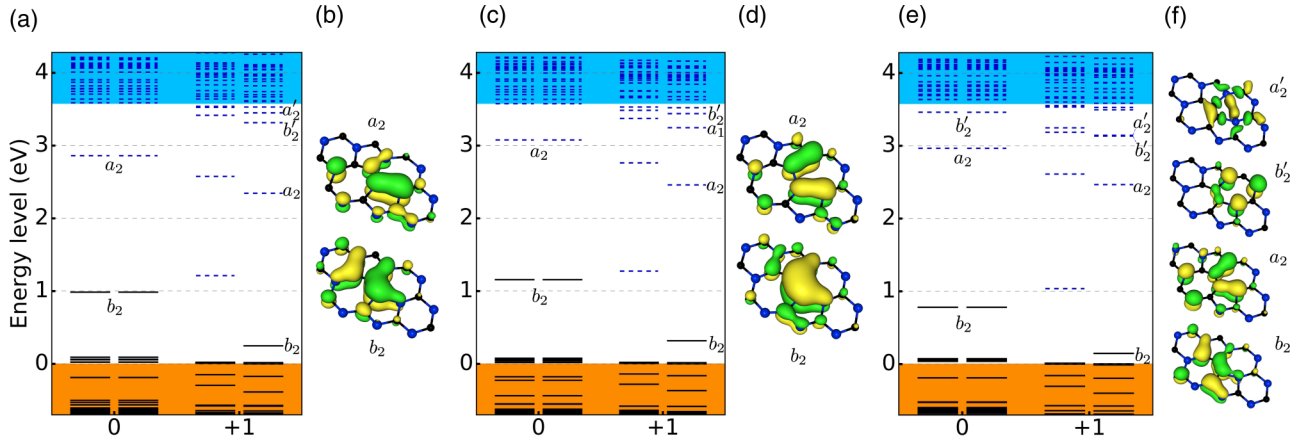


FIG. 4. Kohn-Sham ground state electronic levels of (a) SW, (c) SW-SiC, and (e) SW-C_{Si} defects. Occupied and unoccupied levels are shown with solid black lines and blue dashed lines. Charge density plots for neutral defect states are displayed in (b) SW, (d) SW-SiC, and (f) SW-C_{Si}. The symmetry of molecular orbitals are shown both next to the energy levels and the charge density plots. The C_{2v} symmetry labels are also used for the SW defect.

pure SW defect has a reduced symmetry of C_s , which results in an increased dipole transition probability. For this reason we expect brighter emissions. However, note that for the sake of clarity we have assigned C_{2v} irr labels to the MOs and the multielectron states in Fig. 2 as well as Fig. 4.

We recalculate the electronic structure of these defects in neutral and positive charge states in an 8×8 supercell. Their electronic structure is shown in Fig. 4. If we take a look at this structure, we will find that all the neutral charge states and all the positive charge states are similar. It is because carbon and silicon belong to the same group in the periodic table of the elements as it was demonstrated in group-IV vacancy color centers in diamond [25]. Localization of charge density plot is also displayed in Fig. 4. It determines electronic defect states in the band gap. In this massive supercell we inspected the defects viability in emitting single photons by evaluating the ZPL energy and the HR factor for every electronic transition. These values were displayed in Table II. The values of DW factor are up to 50% in the 2D-SiC monolayer. It confirms the high quantity of these defects in producing single photons. We should mention that these values would be considerably higher in a multilayer of 2D-SiC because the van der Waals forces between layers decrease the structural changes during the excitation, which leads to higher amounts of DW factor. This difference was also observed in hexagonal boron nitride [38]. In Table II the ZPL energies range from 1.4 to 3.3 eV. It demonstrates that observation of single photons would be possible in visible and near-infrared regions which makes

them promising candidates with quantum functionalities in quantum communication, quantum information processing, and biological sensing. For every defect we also plotted the PL spectrum of the transition with the lowest value of the HR factor, which is shown by red color in Fig. 5. The PL spectrum can provide a support for the future experimental investigation of single-photon sources which is related to Stone-Wales defects in 2D-SiC.

Finally, it is worth mentioning that usually the 2D structures of materials are grown on or transformed onto proper substrates [39–41]. Hence, including the effect of substrate surface on the SPEs demands further investigations, which remains an open subject for future studies. We note here that recent calculations on color centers in hexagonal boron nitride have demonstrated that the number of boron nitride layers has minimal effect on the ZPL of the color centers [36]. Similarly, we expect that 2D-SiC monolayers form weak bonds with the substrate, and thus only cause slight modification in the properties of the localized defect states. Experimental techniques alongside proper choice of substrate could be envisaged for diminishing such surface interactions. For instance, oxidation of bilayer silicene on Ag(111) surface leads to a top layer of silicene which has negligible interaction with the substrate [42]. Also, the intrinsic properties of silicene are accessible by epitaxially growing silicene on metal substrates and then transferring it to an insulating substrate [43]. Therefore, in the case of 2D-SiC, as a hypothetical material with properties similar to silicene, once fabricated upon a proper

TABLE II. The ZPL energy, Huang-Rhys, and Debye-Waller factors of Stone-Wales defects for the first, second, and third excitations in an 8×8 supercell.

Defect	First (eV)	HR	DW	Second (eV)	HR	DW	Third (eV)	HR	DW
SW ⁰	1.40	0.94	39%	—	—	—	—	—	—
SW ⁺	1.60	1.23	29%	2.65	2.16	12%	3.26	2.43	9%
SW-SiC ⁰	1.50	0.74	48%	—	—	—	—	—	—
SW-SiC ⁺	1.71	0.93	39%	2.61	1.10	33%	2.64	11.23	0%
SW-C _{Si} ⁰	1.62	1.43	24%	1.45	26.83	0%	2.28	2.39	9%
SW-C _{Si} ⁺	1.72	1.71	18%	1.80	9.50	0%	2.56	3.32	4%

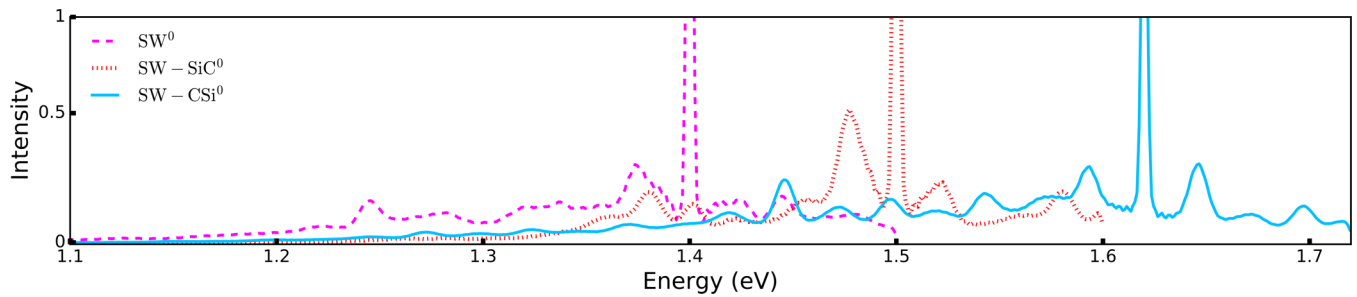


FIG. 5. Photoluminescence line shape of the first excitation of neutral Stone-Wales defects.

substrate with a small interaction our results apply with slight modifications. In fact, if the 2D-SiC layer does not form any covalent bond to the substrate or it floats on another 2D-SiC layer, then the effect on the ZPL position would be minimal because the defect states are really localized in the sheet of 2D-SiC.

IV. CONCLUSION AND OUTLOOK

Our first-principles calculation has led us to introduce the most probable single-photon emitter candidates in two-dimensional SiC monolayer. We calculated the ZPL energy, the Huang-Rhys factor, and the photoluminescence spectrum for some selected defects. The values of the HR factor are in the range of 0.74 to 3.32 (Debye-Waller factor of 48% to 4%). Our *ab initio* analysis demonstrated that Stone-Wales defects (SW, SW-SiC, SW-CSi) in neutral and positive charge states are capable of emitting single photons. The group theory analysis for the SW neutral and charged defects predicted the polarization of radiative and nonradiative transitions, respectively. Increasing dipole transition probability in pure SW defect with lower symmetry convinced us of having brighter emissions in these defects. Our analysis on the spin-orbit interaction suggests that nonradiative transition through the shelving states is also possible. The plotted PL spectra of the transitions with the highest value of the HR factor suggest the following opportunities for future experimental inves-

tigation of single-photon sources which are related to the Stone-Wales defects in 2D-SiC.

In this article a novel two-dimensional material is proposed as a host for single-photon sources and actively encourages other scientific groups who are interested in SPEs field to endeavor for the fabrication of 2D-SiC and explore other fascinating properties of this material. We find that typical defects in 2D materials, Stone-Wales defects, are promising quantum emitters in 2D-SiC which may direct researchers to seek other bright emitters in this material. We note that the presence of metastable triplet states may be harnessed as quantum bits in the neutral Stone-Wales defects but further investigations are required to study this phenomenon in Stone-Wales defects and other potential quantum bits in 2D-SiC.

ACKNOWLEDGMENTS

The authors gratefully acknowledge the Sheikh Bahaei National High Performance Computing Center (SBNHPCC) for providing computing facilities. SBNHPCC is supported by the scientific and technological department of the presidential office and Isfahan University of Technology (IUT). We gratefully acknowledge the help provided by Gergő Thiering. Q.H. thanks Seyed Javad Hashemifar for insightful discussions. A.G. acknowledges the National Quantum Technology Program and National Excellence Program (Projects No. 2017-1.2.1-NKP-2017-00001 and No. KKP129866). M.A. acknowledges support by INSF (Grant No. 98005028).

-
- [1] M. Toth and I. Aharonovich, *Annu. Rev. Phys. Chem.* **70**, 123 (2019).
 - [2] T. T. Tran, S. Choi, J. A. Scott, Z.-Q. Xu, C. Zheng, G. Seniutinas, A. Bendavid, M. S. Fuhrer, M. Toth, and I. Aharonovich, *Adv. Opt. Mater.* **5**, 1600939 (2017).
 - [3] C. Palacios-Berraquero, D. M. Kara, A. R. P. Montblanch, M. Barbone, P. Latawiec, D. Yoon, A. K. Ott, M. Loncar, A. C. Ferrari, and M. Atatüre, *Nat. Commun.* **8**, 15093 (2017).
 - [4] Y.-M. He, G. Clark, J. R. Schaibley, Y. He, M.-C. Chen, Y.-J. Wei, X. Ding, Q. Zhang, W. Yao, X. Xu, C.-Y. Lu, and J.-W. Pan, *Nat. Nanotechnol.* **10**, 497 (2015).
 - [5] P. Tonndorf, S. Schwarz, J. Kern, I. Niehues, O. D. Pozo-Zamudio, A. I. Dmitriev, A. P. Bakhtinov, D. N. Borisenko, N. N. Kolesnikov, A. I. Tartakovskii, S. M. de Vasconcellos, and R. Bratschitsch, *2D Mater.* **4**, 021010 (2017).
 - [6] A. Branny, G. Wang, S. Kumar, C. Robert, B. Lassagne, X. Marie, B. D. Gerardot, and B. Urbaszek, *App. Phys. Lett.* **108**, 142101 (2016).
 - [7] C. Chakraborty, K. M. Goodfellow, and A. N. Vamivakas, *Opt. Mater. Express* **6**, 2081 (2016).
 - [8] I. Aharonovich and M. Toth, *Science* **358**, 170 (2017).
 - [9] S. Ali, M. Ford, and J. Reimers, *Rep. Prog. Phys.* **83**, 044501 (2020).
 - [10] I. Aharonovich, S. Castelletto, D. A. Simpson, C.-H. Su, A. D. Greentree, and S. Praver, *Rep. Prog. Phys.* **74**, 076501 (2011).

- [11] A. Lohrmann, B. C. Johnson, J. C. McCallum, and S. Castelletto, *Rep. Prog. Phys.* **80**, 034502 (2017).
- [12] S. Castelletto, B. C. Johnson, V. Ivády, N. Stavrias, T. Umeda, A. Gali, and T. Ohshima, *Nat. Mater.* **13**, 151 (2013).
- [13] I. A. Khramtsov, A. A. Vyshnevyy, and D. Y. Fedyanin, *npj Quantum Inf.* **4**, 15 (2018).
- [14] S. S. Lin, *J. Phys. Chem. C* **116**, 3951 (2012).
- [15] A. Szabo and A. Gali, *Phys. Rev. B* **80**, 075425 (2009).
- [16] S. Chabi, H. Chang, Y. Xia, and Y. Zhu, *Nanotechnology* **27**, 075602 (2016).
- [17] S. Lin, S. Zhang, X. Li, W. Xu, X. Pi, X. Liu, F. Wang, H. Wu, and H. Chen, *J. Phys. Chem. C* **119**, 19772 (2015).
- [18] T. Susi, V. Skákalová, A. Mittelberger, P. Kotrusz, M. Hulman, T. J. Pennycook, C. Mangler, J. Kotakoski, and J. C. Meyer, *Sci. Rep.* **7**, 4399 (2017).
- [19] Z. Shi, Z. Zhang, A. Kutana, and B. I. Yakobson, *ACS Nano* **9**, 9802 (2015).
- [20] G. Kresse and J. Furthmüller, *Phys. Rev. B* **54**, 11169 (1996).
- [21] J. P. Perdew, K. Burke, and M. Ernzerhof, *Phys. Rev. Lett.* **77**, 3865 (1996).
- [22] J. Heyd, G. E. Scuseria, and M. Ernzerhof, *J. Chem. Phys.* **118**, 8207 (2003).
- [23] A. V. Krukau, O. A. Vydrov, A. F. Izmaylov, and G. E. Scuseria, *J. Chem. Phys.* **125**, 224106 (2006).
- [24] P. Deák, B. Aradi, T. Frauenheim, E. Jánzén, and A. Gali, *Phys. Rev. B* **81**, 153203 (2010).
- [25] G. Thiering and A. Gali, *Phys. Rev. X* **8**, 021063 (2018).
- [26] B. Kaduk, T. Kowalczyk, and T. Van Voorhis, *Chem. Rev.* **112**, 321 (2012).
- [27] P. E. Blöchl, *Phys. Rev. B* **50**, 17953 (1994).
- [28] O. Bengone, M. Alouani, P. Blöchl, and J. Hugel, *Phys. Rev. B* **62**, 16392 (2000).
- [29] Y. Zhang, *J. Semicond.* **40**, 091102 (2019).
- [30] A. Alkauskas, B. B. Buckley, D. D. Awschalom, and C. G. V. de Walle, *New J. Phys.* **16**, 073026 (2014).
- [31] A. Gali, T. Demján, M. Vörös, G. Thiering, E. Cannuccia, and A. Marini, *Nat. Commun.* **7**, 11327 (2016).
- [32] H.-P. Komsa, T. T. Rantala, and A. Pasquarello, *Phys. Rev. B* **86**, 045112 (2012).
- [33] C. Freysoldt, J. Neugebauer, and C. G. Van de Walle, *Phys. Rev. Lett.* **102**, 016402 (2009).
- [34] M. H. Naik and M. Jain, *Comput. Phys. Commun.* **226**, 114 (2018).
- [35] M. Abdi, J.-P. Chou, A. Gali, and M. B. Plenio, *ACS Photon.* **5**, 1967 (2018).
- [36] S. Li, J.-P. Chou, A. Hu, M. B. Plenio, P. Udvarhelyi, G. Thiering, M. Abdi, and A. Gali, *npj Quantum Inf.* **6**, 85 (2020).
- [37] M. Vörös and A. Gali, *J. Comput. Theor. Nanosci.* **9**, 1906 (2012).
- [38] T. T. Tran, K. Bray, M. J. Ford, M. Toth, and I. Aharonovich, *Nat. Nanotechnol.* **11**, 37 (2015).
- [39] B. Feng, Z. Ding, S. Meng, Y. Yao, X. He, P. Cheng, L. Chen, and K. Wu, *Nano Lett.* **12**, 3507 (2012).
- [40] L. Meng, Y. Wang, L. Zhang, S. Du, R. Wu, L. Li, Y. Zhang, G. Li, H. Zhou, W. A. Hofer, and H.-J. Gao, *Nano Lett.* **13**, 685 (2013).
- [41] T. P. Kaloni, M. Tahir, and U. Schwingenschlögl, *Sci. Rep.* **3**, 3192 (2013).
- [42] Y. Du, J. Zhuang, J. Wang, Z. Li, H. Liu, J. Zhao, X. Xu, H. Feng, L. Chen, K. Wu, X. Wang, and S. X. Dou, *Sci. Adv.* **2**, e1600067 (2016).
- [43] L. Tao, E. Cinquanta, D. Chiappe, C. Grazianetti, M. Fanciulli, M. Dubey, A. Molle, and D. Akinwande, *Nat. Nanotechnol.* **10**, 227 (2015).